

June 8, 2022

Physics objects for top quark physics in ATLAS

RICHARD HAWKINGS¹*CERN, EP department, CH-1211 Geneva 23, Switzerland*

Top quark physics measurements performed using data from the ATLAS detector at the LHC rely on efficient reconstruction and precise calibration of leptons, jets and missing transverse energy. A review of the techniques used to reconstruct such objects is given, with an emphasis on the uncertainties achieved for energy calibration and efficiency measurements, illustrated with their impact on key top quark physics results.

PRESENTED AT

9th International Workshop on Top Quark Physics
Olomouc, Czech Republic, September 19–23, 2016

¹On behalf of the ATLAS Collaboration

1 Introduction

The study of events containing top quark pairs ($t\bar{t}$) or single top quarks forms a key part of the ATLAS [1] proton–proton (pp) physics program at the CERN Large Hadron Collider (LHC). Within the Standard Model, 99.8% of top quarks decay into a W boson and b quark ($t \rightarrow Wb$), so the final states are determined by the decay modes of the W boson: leptonic decays $W \rightarrow \ell\nu$ with the lepton ℓ being an electron, muon or tau, or hadronic decays $W \rightarrow q\bar{q}$ with the quarks giving rise to two collimated jets of hadrons in the detector. The reconstruction of leptons, jets (including those tagged as originating from b quarks), and the missing transverse energy from neutrinos produced in $W \rightarrow \ell\nu$ decays, is therefore crucial in fully exploiting the potential of the LHC for top quark physics.

Table 1 shows the data samples delivered by the LHC to ATLAS so far at different centre-of-mass energies \sqrt{s} ; nearly 6M $t\bar{t}$ pairs were produced during Run-1 ($\sqrt{s} = 7\text{--}8$ TeV), and over 30M are now available at $\sqrt{s} = 13$ TeV from Run-2. These samples come with increasing numbers of simultaneous pp collisions per bunch-crossing (pileup), posing significant challenges for the reconstruction of the high transverse-momentum (p_T) objects produced in top quark decays.

Year	\sqrt{s} (TeV)	$\langle \mu \rangle$	L_{int} (fb $^{-1}$)	$\sigma_{t\bar{t}}$ (pb)	$N(t\bar{t})$
2011	7	9	4.6	170	800k
2012	8	20	20.2	250	5M
2015	13	14	3.2	830	2.6M
2016	13	25	33.3	830	28M

Table 1: Data samples available for top physics studies in ATLAS, showing the year and centre-of-mass energy \sqrt{s} , average number of interactions per crossing $\langle \mu \rangle$, integrated luminosity L_{int} , $t\bar{t}$ production cross-section $\sigma_{t\bar{t}}$, and approximate number of $t\bar{t}$ events in each sample.

2 Leptons

Electrons are identified from a shower in the electromagnetic calorimeter, spatially matched to a track reconstructed in the inner detector [2]. The major backgrounds from misidentified hadrons and photon conversions are reduced via cuts on calorimeter shower shapes, matching between the calorimeter energy and track momentum, the detection of transition radiation in the TRT straw-tube tracker, and the presence of a track hit in the first layer of the pixel detector, giving efficiencies of 80-95% for electrons with $p_T > 25$ GeV. Muons are reconstructed from tracks found independently in the inner detector and muon spectrometer, which are then tested for compatibility and combined with a global track fit. This gives an efficiency above

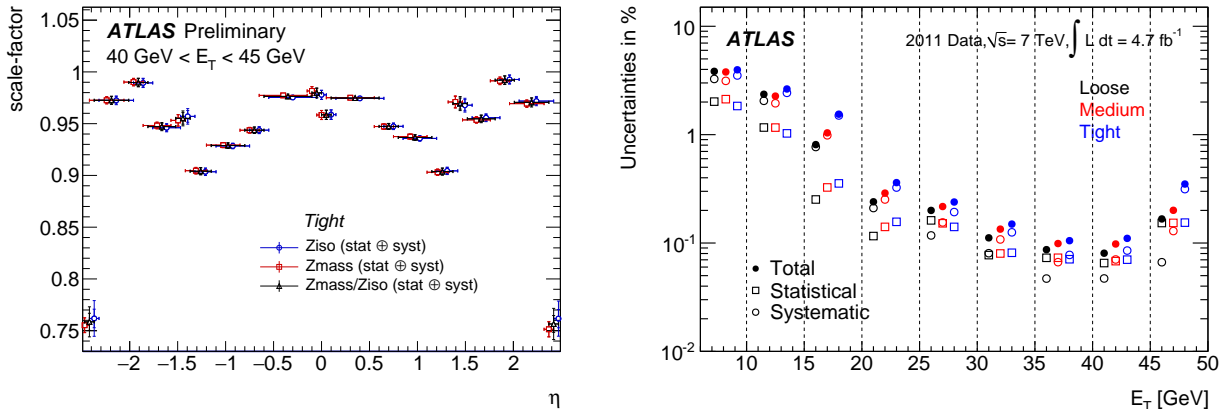


Figure 1: (left) Electron identification efficiency scale factors measured from $Z \rightarrow ee$ tag-and-probe analysis at $\sqrt{s} = 13$ TeV [4]; (right) uncertainties on electron efficiency scale factors at $\sqrt{s} = 7$ TeV [2].

98% for $p_T > 25$ GeV whilst strongly suppressing the background from π/K decays in flight and punch-through of showers from the hadronic calorimeter [3].

The identification efficiencies for both lepton types are measured using the tag-and-probe technique applied to $Z \rightarrow \ell\ell$, $W \rightarrow e\nu$ and $J/\psi \rightarrow \ell\ell$ ($\ell = e, \mu$) decays, requiring one lepton (the tag) to pass tight trigger and identification requirements, and using the resonance mass distribution to determine the background in the other (probe) lepton sample without applying the identification requirements. The efficiencies are measured as functions of lepton p_T and pseudo-rapidity η , and expressed as scale factors with respect to the predictions from simulation. For electrons, the scale factors are typically within 5% of unity (except in regions with large amounts of material in front of the electromagnetic calorimeter) and measured to a precision well below 1% (Figure 1). For muons the scale factors are within 1% of unity and measured with similar precision. The same $Z \rightarrow \ell\ell$ samples are used to provide in-situ corrections to the electron energy and muon momentum scales, using the known value of the Z -boson mass. The width of the reconstructed $Z \rightarrow \ell\ell$ mass distribution is sensitive to the energy/momentum resolution, and used to adjust the resolution in simulation to better model the data, as shown for muons in Figure 2. The uncertainties on the energy/momentum scales are typically smaller than 10^{-3} in the region close to the Z resonance, but some extrapolation to higher energy/momentum is needed to cover the leptons produced in top quark decays.

Leptons from W decays in top events are typically isolated from other hadronic activity, so the sums of calorimeter energy deposits (after correction for pileup) and track momenta close to the leptons are required to be small. These selections reject leptons from semi-leptonic decays of heavy flavour hadrons. Leptons also provide efficient triggers for selecting top events online, with efficiencies for $p_T > 25$ GeV

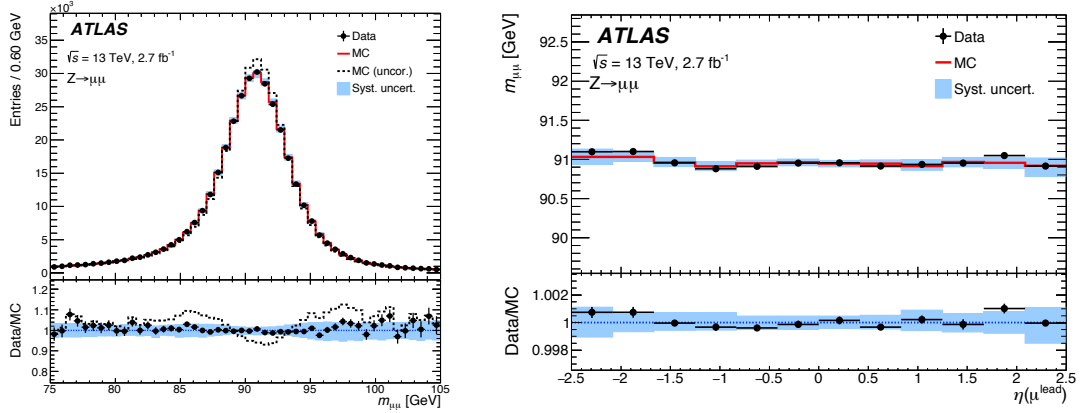


Figure 2: (left) Di-muon invariant mass distribution for selected $Z \rightarrow \mu\mu$ events compared to uncorrected and corrected simulation with systematic uncertainty; (right) stability of mean reconstructed mass vs. η of the highest p_T muon [3].

above 90% for electrons and 70-85% for muons, limited by the geometrical coverage of the trigger chambers. Dilepton events are typically selected with a logical OR of single lepton triggers, providing a robust trigger with 99% per-event efficiency, and small systematic uncertainties, again measured using Z tag-and-probe techniques.

The uncertainties from limited knowledge of lepton efficiencies and calibration in the ATLAS $t\bar{t}$ inclusive cross-section measurements from $e\mu$ dilepton events at $\sqrt{s} = 7, 8$ and 13 TeV [5] are shown in Table 2. These are all well below 1% (even in the less mature $\sqrt{s} = 13$ TeV analysis) and significantly smaller than the leading uncertainties from $t\bar{t}$ modelling and luminosity measurement.

3 Jet, b -tagging and missing transverse energy

The outgoing quarks and gluons from the hard-scattering collision are reconstructed as collimated jets of hadrons in the detector. ATLAS uses the anti- k_T jet algorithm applied to topological clusters of energy deposits in the calorimeters. The simulation-based jet energy scale calibration is augmented with data-based corrections exploiting energy balance in photon+jet, Z +jet and multijet events [7]. The resulting systematic uncertainties as a function of jet p_T are shown in Figure 3 (left); uncertainties of below 2% for $p_T = 100$ GeV have already been achieved in Run-2 data, with up to a factor two better being achieved in Run-1. Jet energy scale uncertainties are typically amongst the leading ones for measurements of jet activity in top events, and in measurements of the top mass, contributing e.g. 0.6 GeV to the top mass uncertainty in the lepton+jets measurement at $\sqrt{s} = 7$ TeV [6].

At high invariant masses of the $t\bar{t}$ system, the top quarks become highly boosted, and the jets from hadronic top decays $t \rightarrow bq\bar{q}$ can no longer be resolved. Jet substructure techniques, in which a large radius ($R = 1.0$) jet capturing all the top quark decay products is broken down to reveal the mass of the heavy object within,

Uncertainty source (%)	7 TeV	8 TeV	13 TeV
Electron efficiency	0.13	0.41	0.3
Electron scale/resolution	0.22	0.51	0.2
Electron isolation	0.59	0.30	0.4
Muon efficiency	0.30	0.42	0.4
Muon scale/resolution	0.14	0.02	< 0.05
Muon isolation	0.44	0.22	0.3
Lepton trigger	0.19	0.16	0.2

Table 2: Lepton-related relative uncertainties (in %) on the measurements of the $t\bar{t}$ production cross-section at $\sqrt{s} = 7, 8$ and 13 TeV [5].

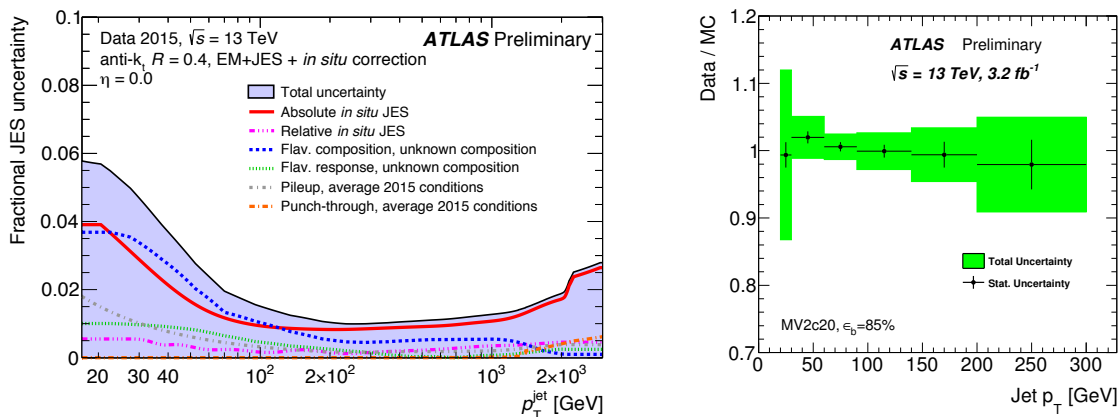


Figure 3: (left) Fractional jet energy scale uncertainty as a function of jet p_T for jets at $\eta = 0$ in 2015 data at $\sqrt{s} = 13$ TeV, illustrating the contributions of the various components [7]; (right) b -tagging efficiency scale factors with statistical and systematic uncertainties measured using $t\bar{t}$ events in $\sqrt{s} = 13$ TeV data [8].

whilst removing the soft contributions from QCD radiation and pileup, are essential in measuring differential cross-sections at high top quark p_T [9].

The identification of jets likely to have originated from b -quarks plays an important role in isolating events containing top quarks (due to the dominant $t \rightarrow Wb$ decay), and assigning jets to top quark decay products when performing kinematic fits. With the addition of the Inner B-Layer pixel detector at $r = 33$ mm from the collision point, the b -tagging efficiency has been boosted in Run-2 compared to Run-1 by around 10% for a similar rejection of light quark, gluon and charm jet background [10]. The b -tagging efficiency is also measured in data by exploiting $t\bar{t}$ events, allowing efficiency scale factors to be derived with a precision of 2–3% for jets in the 50–150 GeV p_T range [8], as shown in Figure 3 (right).

The neutrinos produced in the leptonic decays of W bosons from top quark decays escape detection and give rise to missing transverse energy (E_T^{miss}), i.e. imbalance in

the vector sum of transverse momentum of all objects in the final state. The E_T^{miss} resolution is affected by the resolution of the soft term, i.e. the residual energy not clustered into jets or electrons. In Run-2, the contribution of pileup to this soft term is minimised by replacing calorimeter energy clusters by tracks reconstructed in the inner detector and associated to the primary vertex from the hard-scattering collision rather than those from pileup interactions. The reconstructed E_T^{miss} can be used to separate top quark events from multijet background, and to help reconstruct the kinematics of the top quark(s) in the event.

4 Outlook

Top physics studies rely on measurements of many of the physics objects ATLAS can reconstruct. The detector, reconstruction and calibration procedures are working well at $\sqrt{s} = 13$ TeV, and uncertainties are beginning to approach those achieved with the Run-1 data. Top analyses are typically limited by the systematic uncertainties related to jets, rather than leptons which can be precisely calibrated using $Z \rightarrow \ell\ell$ decays. Jet substructure techniques are also beginning to bear fruit, and ATLAS looks forward to more data and top quark physics results in the next few years.

References

- [1] ATLAS Collaboration, JINST 3 (2008) S08003.
- [2] ATLAS Collaboration, Eur. Phys. J. C74 (2014) 2941, arXiv:1404.2240.
- [3] ATLAS Collaboration, Eur. Phys. J. C76 (2016) 292, arXiv:1603.05598.
- [4] ATLAS Collaboration, ATLAS-CONF-2016-024.
- [5] ATLAS Collaboration, Eur. Phys. J. C73 (2014) 3109, arXiv:1406.5375;
ATLAS Collaboration, Phys. Lett. B761 (2016) 136, arXiv:1606.02699.
- [6] ATLAS Collaboration, Eur. Phys. J. C75 (2015) 330, arXiv:1503.05427.
- [7] ATLAS Jet/ETMiss group public results:
<https://twiki.cern.ch/twiki/bin/view/AtlasPublic/JetEtmissPublicResults>
- [8] ATLAS flavour tagging group public results: <https://twiki.cern.ch/twiki/bin/view/AtlasPublic/FlavourTaggingPublicResultsCollisionData>
- [9] ATLAS Collaboration, ATLAS-CONF-2016-040.
- [10] ATLAS Collaboration, ATLAS-PHYS-PUB-2015-022.